urban science

Article

Biodiesel Production by Transesterification of Recycled Oil Catalyzed with Zinc Oxide Prepared Starting from Used Batteries

Domenica Seminario-Calle [1,†], Melissa Ortega-Maldonado [1,†], Verónica Pinos-Vélez [1,2,*], Juan Cisneros [2], Andrés Montero-Izquierdo [1], Paulina Echeverría-Paredes [1], Paola Duque-Sarango [2,3] and Paúl Álvarez-Lloret [1]

[1] Grupo de Ingeniería de las Reacciones Químicas, Catálisis y Tecnologías del Medio Ambiente (IRCMA), Bioscience Department, Universidad de Cuenca, Víctor Manuel Albornoz, Cuenca 010107, Ecuador; domenica.seminario@ucuenca.edu.ec (D.S.-C.); isabel.ortega06@ucuenca.edu.ec (M.O.-M.); andres.montero@ucuenca.edu.ec (A.M.-I.); paulina.echeverria@ucuenca.edu.ec (P.E.-P.); paul.alvarez@ucuenca.edu.ec (P.Á.-L.)
[2] Departamento de Recursos Hídricos y Ciencias Ambientales, Universidad de Cuenca, Víctor Manuel Albornoz, Cuenca 010107, Ecuador; juan.cisneros@ucuenca.edu.ec (J.C.); pduque@ups.edu.ec (P.D.-S.)
[3] Grupo de Investigación en Recursos Hídricos (GIRH-UPS), Universidad Politécnica Salesiana, Campus El Vecino, Calle Vieja 12-30 y Elia Liut, Cuenca 010203, Ecuador
* Correspondence: veronica.pinos@ucuenca.edu.ec
† These authors contributed equally; thus, both share the first authorship.

Abstract: The consumption of batteries and cooking oil have been increasing. Most used batteries are disposed of incorrectly, leading to health and environmental problems because of their composition. In a similar form, cooking oil, once used, is often released by the discharge reaching the wastewater, polluting soil, and water, which affects its treatment. In Ecuador, these environmental passives are recollected and stored without further treatment, which is a temporary and unsustainable solution. To address this issue, the circular economy concept has gained increasing attention. In this study, zinc oxide was prepared from discarded batteries using the hydrometallurgical method to use as a catalyst; it achieved 98.49% purity and 56.20% yield and 20.92% of particles presented a particle size of 1–10 nm. Furthermore, the catalyst morphology was investigated in an SEM, which showed that particle size ranged from 155.69 up to 490.15 nm and spherical shapes. Due to its characteristics, the obtained catalyst can be used in the industry instead of the zinc oxide obtained by mining processes. These processes are known to produce heavy contamination in the ecosystems and human health. Additionally, a zinc oxide lifecycle in the environment was analyzed through a material flow analysis (MFA), taking into consideration two paths, one assuming the disposal of used batteries and the other assuming the recycling of zinc. Biodiesel was produced with a heterogeneous catalyst. This took place with a transesterification reaction with used cooking oil, ethanol, and zinc oxide (ZnO) as catalysts. The biodiesel obtained had the following characteristics: 37.55 kJg^{-1} of heating power, 0.892 gcm^{-3} of density, 4.189 mm^2/s of viscosity, 0.001% of water content, and a 70.91% yield. Furthermore, the energy consumption in biodiesel production was quantified, giving a total of 37.15 kWh. This kind of initiative prevents that waste from becoming environmental pollutants and potential health risks by giving them a second use as a resource. Moreover, turning waste into a valuable product makes the processes self-sustaining and attractive to be implemented.

Keywords: biodiesel; circular economy; discarded zinc batteries; used cooking oil; zinc oxide

check for updates

Citation: Seminario-Calle, D.; Ortega-Maldonado, M.; Pinos-Vélez, V.; Cisneros, J.; Montero-Izquierdo, A.; Echeverría-Paredes, P.; Duque-Sarango, P.; Álvarez-Lloret, P. Biodiesel Production by Transesterification of Recycled Oil Catalyzed with Zinc Oxide Prepared Starting from Used Batteries. *Urban Sci.* **2023**, *7*, 80. https://doi.org/10.3390/urbansci7030080

Academic Editors: Luis Hernández-Callejo, Marcia Eugenio-Gozalbo, Yu-Sheng Shen, Tigran Haas, Pablo de Frutos Madrazo and Sergio Nesmachnow

Received: 27 May 2023
Revised: 5 July 2023
Accepted: 17 July 2023
Published: 31 July 2023

1. Introduction

Most batteries, alkaline and Zn-C, which are used as power sources of energy for electronic devices, are not disposable. In recent years, in Ecuador, there has been an increase in battery consumption. A study in Ecuador in 2020 found that the national population of 16.8 million inhabitants consumes 17 million batteries, representing a per

capita consumption of 1.06 $kghab^{-1}$. Only 1.53 million of these batteries were rechargeable (9.06%) [1]. It is estimated that 78.15% of the population dispose of batteries in common garbage, 6.08% burn or bury them, 5.95% keep them in their house, and only 8.21% deposit them in the proper collection center. This disposal practice leads to the accumulation of batteries in city landfills and results in pollution problems, particularly in water sources and soil, due to the leachates containing heavy metals [2–4].

The Ecuadorian Institute of Standardization (INEN) establishes that used batteries in Ecuador must be handed over to professionals authorized by the Ministry of Environment or AAAR (Responsible Environmental Enforcement Authority), according to the INEN 2534 standard. The process to be followed from collection to recycling is also outlined by the INEN [5]. However, unlike in Europe, where directives prohibit the disposal of batteries through incineration or dumping, there is no law in Ecuador prohibiting these methods [6]. In the city of Cuenca, although EMAC is the public company in charge of garbage collection, it lacks the initiative to collect batteries separately from other types of waste. In this regard, ETAPA EP (the public company responsible for water treatment and distribution) has assumed the responsibility of preventing batteries from contaminating drinking water sources and the wastewater treatment plant; however, its action is limited [7]. ETAPA EP collection points gather approximately 35–40 kg of batteries each month. After conducting a stabilization process, the batteries are confined [7]. This strategy entails logistical problems such as a lack of space and potential hazards, including the possibility of metal leaching due to flooding.

An effective waste management program should aim to provide batteries with a final treatment that needs to be environmentally sustainable and cost-effective. A typical alkaline battery comprises a zinc anode and a high-density manganese oxide cathode (MnO_2). In contrast, Zn-C batteries are predominantly made of zinc, followed by MnO_2. Then, from this composition, around 33% of zinc and 29% of manganese oxide can be recovered and used as raw material for industry [8]. Some authors have even succeeded in obtaining zinc oxide from Zn-C batteries. For instance, one study used sulfuric acid (H_2SO_4) for reductive leaching and selective precipitation with NaOH at pH 10 [9]. In contrast, another used an ionic liquid for battery leachate treatment [4]. Additionally, a third study employed solvent extraction, electrodeposition, and precipitation methods [10].

Currently, zinc oxide production mainly relies on chemical processes that utilize zinc as the raw material. Unfortunately, zinc is often mined alongside other metals, particularly lead, resulting in significant pollution with toxic metals in soil, water, and sediments from Pb-Zn mines [11]. Mining activities also lead to a substantial release of heavy metals into the environment, with zinc alone contributing up to 1.38×10^6 $kgyear^{-1}$ in close mining regions [12]. Such releases have been shown to cause freshwater and marine human toxicity, ecotoxicity, metal depletion, eutrophication, and soil damages [13]. Zinc is an essential element in the human body. Nevertheless, its excessive intake causes stomach cramps, nausea, and vomiting, and long-term exposure can affect cholesterol balance, immune system function, and fertility [12]. Additionally, heavy metals that incorporate into the soil can decrease pH, nutrients, and microbial diversity, rendering them unsuitable for agriculture since they leach into water bodies [12,14]. China, the biggest supplier of zinc in the world, has several regions next to mines with contaminated soil and water, leading to health issues for residents [12]. Poland has also contaminated allotment gardens in closed Zn and Pb mines, with the concentration of metals in soil and crops exceeding European Quality Standards, resulting in the integration of these contaminants into the food chain [14]. In Ecuador, mining areas have high concentrations of Zn in nearby rivers, with levels ranging from 513–2670 $mgkg^{-1}$. This is due to the discharge of waste generated during gold and silver extraction processes into the rivers, which carry heavy metals such as zinc [15]. Furthermore, ecosystem remediation from Zn-Pb mines can cost up to $\$ 3.04 \times 10^{10}$ [16].

Another common waste product is cooking oil. It is often taken to be inoffensive; nevertheless, its inadequate disposal can cause significant environmental harm. Typically, it is

poured down the drain, leading to contamination of water bodies and wastewater treatment plants, negatively affecting the ecosystem and water treatment efficiency, respectively [17]. The oil forms a layer on the water that obstructs sunlight and limits oxygen absorption, leading to additional ecosystem damage. Additionally, removing oil from wastewater can be expensive [18]. In Ecuador, ~54 million liters of discarded oil are generated, and ~70% of this waste comprises vegetable oil [1]. ETAPA EP is responsible for collecting and managing this waste to avoid water contamination. Still, this action is limited to collecting and storing the oil and, in some cases, transferring it if an individual or institution requires it. Storing the oil is not a definitive solution because, in addition to the space problem, there is, as in the case of batteries, the danger of infiltration where the oil can leak [19]. However, there are ways to revalue this waste, such as producing biodiesel [20]. This is produced by transesterification, where used cooking oil triglycerides chemically react with alcohol to form fatty acid methyl esters [21], see Figure 1.

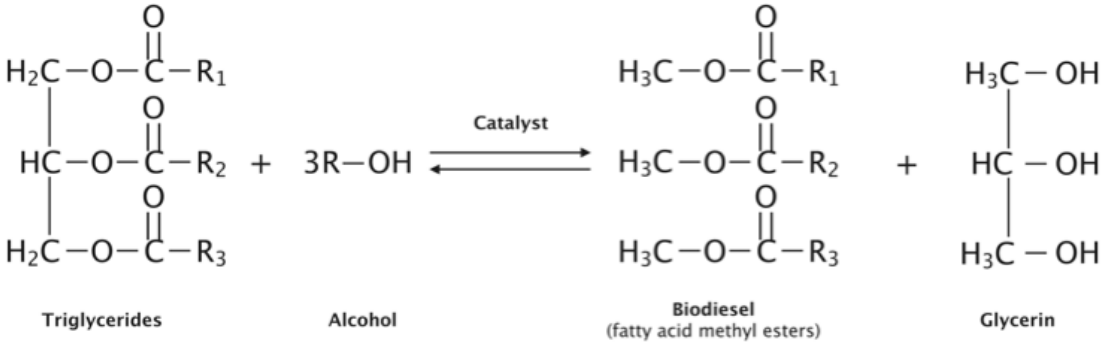

Figure 1. Transesterification reaction.

As shown in Table 1 (Inputs 1 to 4), biodiesel production has been extensively studied using homogeneous catalysts. This type of reaction is characterized by being fast, with a yield of over 90%. Nevertheless, it has disadvantages such as loss of catalyst and the need for neutralization. Table 1 also displays several investigations on biodiesel production utilizing different heterogeneous catalysts, along with 1% or less of the catalyst. The results indicate that the reaction is highly efficient, with the advantage of recovering the catalyst. Nevertheless, the reaction is a little slower in some cases due to diffusional mass problems. One of the catalysts used for the transesterification reaction is zinc oxide, indicated in Table 1 (Inputs 6 and 7). The use of discarded batteries' zinc oxide and used cooking oil for producing biodiesel can effectively reduce the amount of hazardous waste and its management costs [22]. Biodiesel is a great candidate to replace fossil fuels as a clean energy source due to its advantages. The main one is that the emission of CO_2, CO, unburned hydrocarbons, and particles is lower compared to fossil fuels. Likewise, the emission of SO_2 during the biodiesel combustion process is lower, due to low sulfur content in the biodiesel raw materials. These emission gases are the main cause of atmospheric pollution. Some other advantages include the fact that biodiesel can be produced from recycled oils and fats, can be used directly in diesel engines, and reduce the dependence on fossil fuels [23,24].

This research explores alternative processes that can properly revalorize waste municipal organic oil and batteries, which currently need to be managed appropriately. The proposed approach involves preparing the zinc oxide from discharged Zn-C batteries by a novel hydrometallurgical method and preparing biodiesel from cooking oil by catalyzed transesterification. Moreover, a material flow analysis (MFA) is developed to analyze the inputs, outputs, and storage of materials during 2022. This work evaluates a real sample of batteries and discarded oil deposited in municipal warehouses contributing to a circular economy, considering the real conditions in which these are delivered. For instance, discarded oil used in this study is a mixture of various sources from the entire city, such as

fast-food stalls, local houses, restaurants, etc. In fast food stalls, a highly saturated oil, due to its reuse, is handed over for recycling.

Table 1. Transesterification condition's reaction to produce biodiesel with waste oil.

Input	Type of Oil	Catalyst		Oil/Alcohol	Reaction Time, min	Yield, %	Ref.
		Type	%				
1	Used Frying Oil from Sunflower	KOH	1	1:6	60	99.3	[25]
2	Waste Cooking Oil	KOH	0.5	1:6	60	93.13	[26]
3	Waste Municipal Organic Oil	KOH	1	1:6	90	93.31	[27]
4	Waste Municipal Organic Oil	NaOH	0.5	1:6	90	85.96	[27]
5	Waste Cooking Oil	CaO	1	1:8	90	96	[28]
6	Refined Palm oil	CaO-ZnO	7.5	1:30	120	86.99	[26]
7	Waste Cooking Oil	CFA/ZnO	0.5	1:12	180	98.14	[29]
8	Waste Cooking Oil	S–TiO_2/SBA-15	1	1:15	30	94.96	[30]

Ethanol was employed as the alcohol in all experiments.

2. Materials and Methods

2.1. Characterization and Pretreatment of Discarded Vegetable Oil

The discarded vegetable oil used in this study was sourced from a public company ETAPA EP in Cuenca, Ecuador. ETAP EP collects discarded oil from restaurants and households to store oil in an open pool. Before analysis, the sample of discarded vegetable oil was filtered through Whatman paper $N_{o.}$ 40 using a glass funnel to remove residues. Next, filtered oil was washed with water at 80 °C, then left in a decanter. After removing the water from the decanter, the discarded vegetable oil was heated at 115 °C for 4 h to remove water. A pycnometer determined the density and Equation (1) was applied, where: ρm: sample density; m_0: empty pycnometer weight; m_1: weight of the pycnometer with water; m_2: weight of the pycnometer with sample; ρ_a: water density.

$$\rho = (m_2 - m_0)/(m_1 - m_0)\rho_a \quad (1)$$

The Ostwald procedure was used to measure the kinematic viscosity at 40 °C, with water as the reference liquid. The process involved placing 10 mL of distilled water in the Ostwald viscometer and immersing it in a container alongside a thermometer. The mixture was then heated until the liquid reached the upper limit A before being allowed to fall to the lower limit B, and the time taken was recorded alongside the temperature. The process was repeated with water at room temperature and the treated oil sample. The viscosity was calculated using the following Equation (2), where: μ: kinematic viscosity; ρ: density; n: dynamic viscosity.

$$\mu = \frac{\rho}{n} \quad (2)$$

The Karl Fischer titration method was employed to determine the water percentage in the sample. The sample was first weighed and then added to the equipment, where an iodine indicator was automatically added while stirring continuously. The platinum electrode determined the endpoint of the titration, and the percentage of water in the sample was displayed once all the water in the sample had been consumed.

2.2. Preparation of Zinc Oxide and Characterization

ETAPA EP provided Zn-C batteries, which were used in this study, see Table 2.

Table 2. Battery components.

Component	Percentage, %
Zinc (anode)	16.86
Manganese dioxide (cathode)	29.00

Table 2. *Cont.*

Component	Percentage, %
Carbon	5.71
Mercury	0.01
Cadmium	0.08
Ammonium chloride (electrolyte)	25.76
Plastic and others	22.76

Initially, only batteries in good condition, without rust or spills, were chosen. Subsequently, the batteries were disassembled. The zinc case and carbon rods were extracted by dismantling used batteries. The rods of carbon were immersed in nitric acid of 30% of concentration for 24 h, followed by washing until achieving a pH~7. Subsequently, the rods were dried at 110 °C for 12 h in an oven to eliminate any remaining water. A pyrometallurgical method was used to obtain zinc oxide [31] and to lixiviate the zinc case. To obtain 195.66 g of zinc chloride, 115.6 g of the zinc case was lixiviated at 100 °C for 60 min with 300 mL of hydrochloric acid of 37% concentration. Subsequently, 250 mL of sulfuric acid at 50% concentration was added. The solution was heated at 100 °C for an hour. In order to eliminate the impurities of the zinc sulfate, 500 mL of distilled water was added. The solution was boiled and filtered through Whatman No. 40 paper. The filtered solution was allowed to cool and stand at room temperature. Finally, crystals of sulfate of zinc (231.53 g) were obtained. To obtain zinc hydroxide (231.53 g) from the sulfate of zinc crystals, sodium hydroxide (Fisher Scientific, USA, assay ≥98.9%) solution of 30% of concentration was added until a pH of 6.5 was reached; as a by-product, sodium sulfate (341.46 g) was obtained. The subproduct, sodium sulfate, produced during the process is of a low concentration and not harmful to health, according to references [32,33]. The zinc hydroxide was recovered by filtration with Whatman paper No. 40, then dried at 100 °C for 1 h. Finally, zinc hydroxide was calcinated in a muffle at 900 °C for 6 h to obtain zinc oxide. The reactions that occurred are presented as follows.

$$ZnO + 2HCl \rightleftharpoons ZnCl_2 + H_20$$

$$ZnCl_2 + H_2SO_4 \rightleftharpoons ZnSO_4 + 2HCl$$

$$ZnSO_4 + 2NaOH \rightleftharpoons 2NaSO_4 + Zn(OH)_2 \downarrow$$

$$Zn(OH)_2 \rightleftharpoons ZnO + H_2O$$

In order to prepare the supported catalyst, zinc oxide (0.96 mg) was dispersed in water at 300 rpm. Then, a dry carbon rod (4.8 g) also recovered from the discarded batteries was impregnated with the oxide at 230 °C to evaporate all the solvent.

Scanning electron microscopy (SEM JEOL IT300) characterized the supported and unsupported zinc oxide characteristics to determine their superficial morphological and structural features. The zinc content was determined using atomic absorption with a graphite furnace (A. Perkin Elmer (Waltham, MA, USA) 3300 spectrometer AA with graphite furnace HGA 600). A structural characterization was held in an X-ray diffractor Bruker, Billerica, MA, USA, D2 Phaser, second generation.

2.3. Biodiesel Preparation and Characterization

The ethanol/oil ratio 6:1 was used for transesterification using both supported (ZnO-C) and unsupported catalysts (ZnO). The catalyst used were 5% $W_{ZnO}W^{-1}_{solution}$ or 1% $W_{ZnO-C}W^{-1}_{solution}$. The ratio of ethanol/oil and the amount of catalyst were established based on the studies shown in Table 1. To prepare the biodiesel, first ethanol (98%) and the catalyst (supported or unsupported) were mixed at 300 rpm, 60 °C for 20 min. Then, cleaned used oil was added and stirred for one hours. The resulting mixture was separated by decantation. After 3 h, the biodiesel was separated from the glycerin. The

diesel was filtered by Whatman paper No. 42 and washed to recover the remaining catalyst. Finally, biodiesel was dried at 80 °C for 15 min. The process was repeated in triplicate for each catalyst type.

The entire process, from the disassembly of the batteries to the preparation of the zinc oxide and the cleaning of the used oil, through the transesterification reaction to obtain biodiesel, is shown in Figure 2.

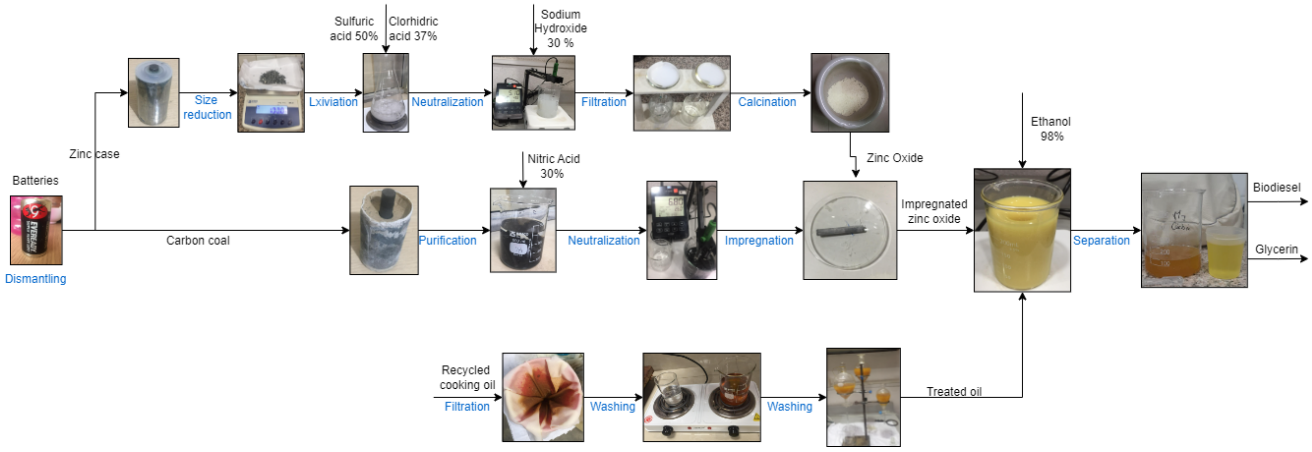

Figure 2. Catalyst obtention and transesterification reaction.

Biodiesel characterization involves the evaluation of five parameters: water content, specific heat capacity, density, viscosity, and reaction yield. The water content was obtained by injecting the sample into a Karl Fischer titrator. The specific heat capacity was achieved through a calorimetric pump. Density was measured by employing the pycnometer method. Viscosity was determined using the Ostwald method with an Ubbelohde viscometer, as described in Section 2.1. The reaction yield was calculated by analyzing the fatty acid methyl esters (FAMEs) for used oil and biodiesel samples. Derivatized samples were analyzed using gas chromatography to determine the concentration of the FAMEs of interest. All parameters were compared to three biodiesel standards: ASTM B 100, EN 590, and INEN 2489 [34–36].

2.4. Material Flow Analysis (MFA)

This analysis focuses on the study of a chemical element, compound, or material based on the law of conservation of mass. It aims to identify key aspects such as origin, volumes, generated waste, and emissions produced. Based on this, decisions can be made regard to resource, waste, and environmental management. In this case, the material to be analyzed is Zn-C batteries. For this purpose, an exhaustive search was conducted to gather information on the quantity of batteries from their commercialization up to their final disposal in the city of Cuenca in the year 2022. The choice of this particular year for analysis is due to the lack of available data on battery consumption between 2020 and 2021, which is attributable to the pandemic. Therefore, data on battery consumption were not collected until the year 2022, as provided by INEN. This information was used to identify flows, stocks, and processes. Once identified, the transfer coefficient was determined, which indicates the fraction of substance or material that enters and leaves a process. Equation (3) was used:

$$CT = \frac{Y1}{\sum X1} \tag{3}$$

where CT: transfer coefficient; $Y1$: process output mass; $X1$: process input mass.

This collected information was used to calculate the mass balance using STAN software. Mass flow data and transfer coefficients were entered into a flow diagram created in the software.

3. Results and Discussion

3.1. Zinc Oxide Characterization

3.1.1. Zinc Oxide Color, Purity, and Yield

A white powder of zinc oxide was obtained after applying the procedure mentioned in Section 2.2. Table 3 displays the results of the catalyst characterization. The purity of the zinc oxide was 98.49%, which is higher than the purity obtained in other studies that used the same hydrometallurgical method [31]. The color of the zinc oxide was white, and the yield obtained was 56.20% [31], which is similar to the yield obtained in this study (54.7%). However, when alkaline batteries were used, the yield was higher (66.42%) according to another study [37]. Finally, the nanometric scale fraction of the sample was 20.92%, indicating no uniform size.

Table 3. Zinc Oxide Characterization.

Characteristic	
Color	White
Purity, %	98.49
Particle size (1–10 nm), %	20.92
Yield, %	56.20

3.1.2. Zinc Oxide Particle Size

The catalyst morphology was investigated using scanning electron microscopy (SEM). Figure 3a displays the morphology of pure zinc oxide particles, while Figure 3b shows the supported zinc oxide. The size of pure ZnO particles ranged from 155.69 nm to 490.15 nm. The zinc oxide particles in Figure 3b exhibited spherical shapes with slight agglomeration deposited over the carbon support.

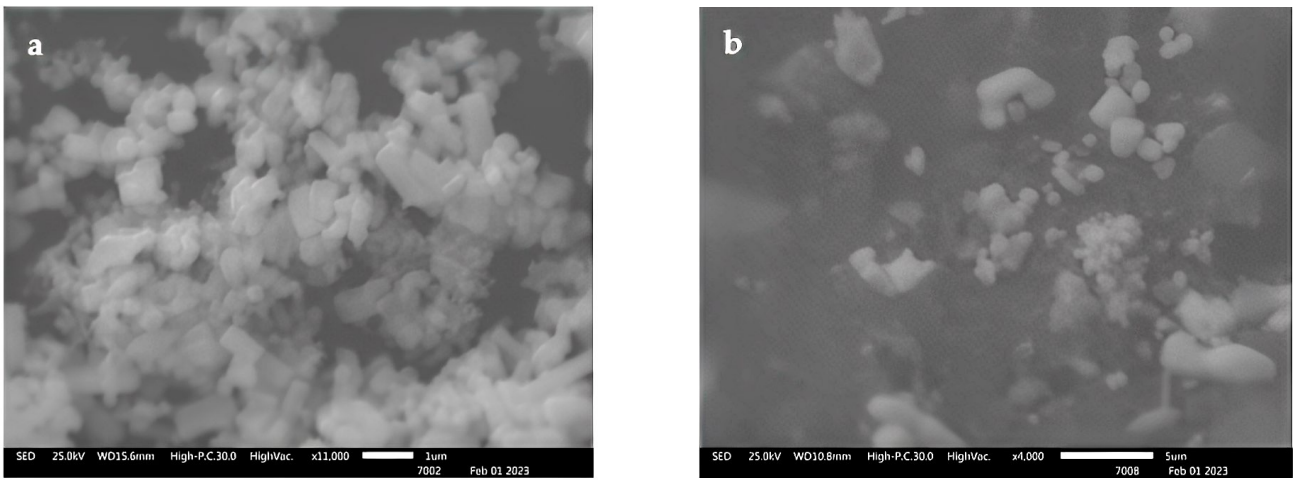

Figure 3. Scanning electron microscopy image of (**a**) zinc oxide particles, (**b**) zinc oxide particles supported in a carbon bar.

3.1.3. XRD Analysis

An structural characterization was held in a BRUKER D2 Phaser second generation X-ray diffractor. Figures 4 and 5 show the diffraction patterns obtained from both the carbon rod-impregnated ZnO and the ZnO−only sample. The presence of zinc oxide is verified in these two figures.

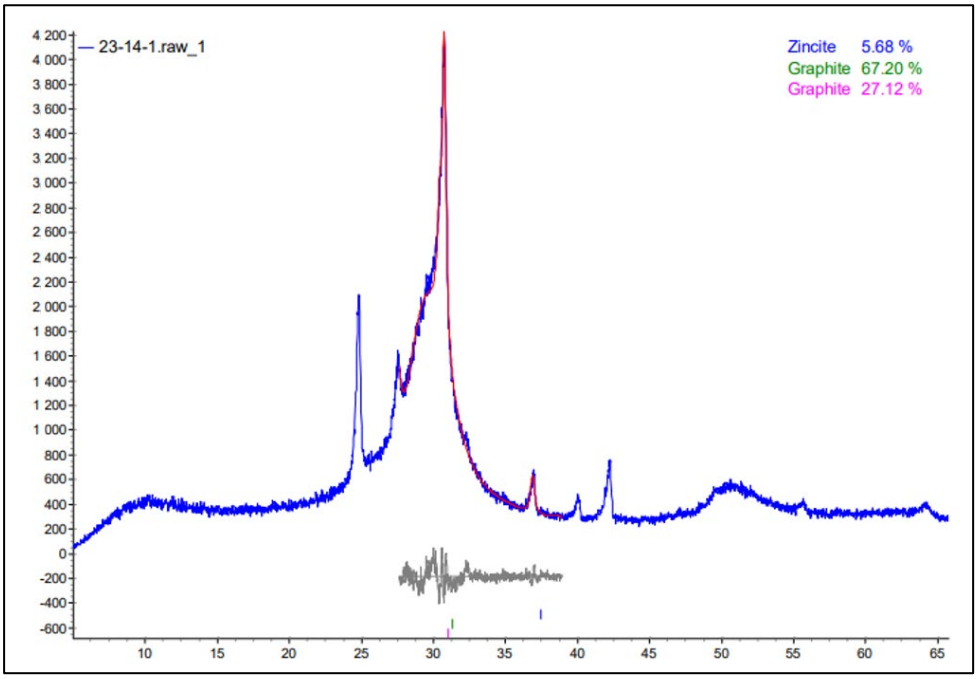

Figure 4. XRD of the ZnO−impregnated carbon bar sample.

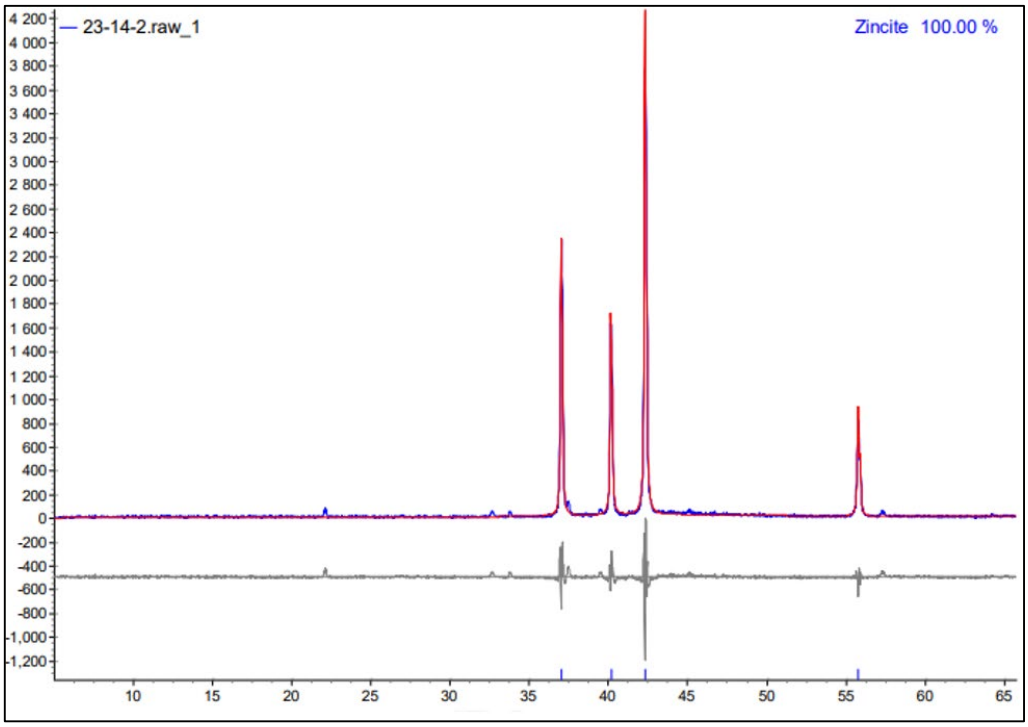

Figure 5. XRD of the ZnO sample. Samples in red and blue in gray the pattern.

The XRD pattern of the impregnated ZnO sample (Figure 4) revealed 5.68% ZnO. While the diffraction pattern of the sample of ZnO (Figure 5) presented a composition of 100% ZnO.

3.1.4. Pore Size and Surface Area

The values of pore volume and surface area are shown in Table 4.

Table 4. Results of coal analysis by BET method.

Description	Value
Surface area, m^2g^{-1}	1.93
Pore volume, cm^3g^{-1}	0.79

According to IUPAC, the pore distribution ranges from macro pores larger than 50 nm, mesopores between 2 to 50 nm, and micropores smaller than 2 nm. In this case, the coal falls under the category of mesopores; see Figure 6.

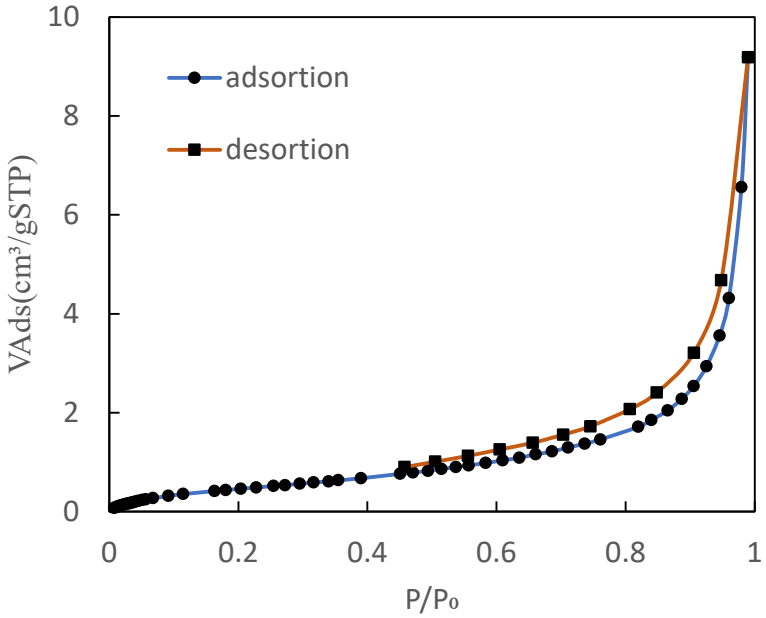

Figure 6. BET Isotherm of coal sample with impregnated ZnO catalyst.

3.2. Material Flow Analysis (MFA)

A material flow analysis was conducted to analyze the zinc oxide movement in the environment. Two diagrams are presented, one assuming the disposal of used batteries (refer to Figure 7), and the other assuming zinc recovery from used batteries (refer to Figure 8).

To conduct the MFA analysis, it was necessary to gather information on the inputs and outputs throughout the importation and commercialization to the final disposal of the batteries. The starting point was the quantity of batteries imported into Ecuador in 2022, which was 2170 tons, according to ITC [38]. According to INEC [39], 79.8% of discarded batteries was disposed of in the trash, 8.2% was burned, 5.6% was stored at home, 4.4% was left at collection centers, and 2% was given away or sold. It is worth noting that these data were collected at the national level, as no specific data were available for the city of Cuenca. Thus, this information was utilized under the assumption that the population of Cuenca exhibits the same consumption and disposal behavior as the national average.

According to Figure 7, after consumption, most of the batteries end up in landfill with 1731.66 t/y, and the rest of the batteries are incinerated or stored at home. EMAC EP is the company in charge of constantly monitoring the physical and chemical properties of the leachate produced at the Pichacay landfill in Cuenca, especially pH and heavy metals such as Zn. The pH can indicate the mobilization of dissolved inorganic species or ion concentrations. The landfill has two leachate zones: North 1 (LN1) and North 2 (LN2). According to the data provided by EMAC EP, the pH taken during 2022 in the LN1 zone ranges from 7.8 to 8.8. This is because the leachates in that zone run off from old and disused cells at the end of the methanogenic or maturation stage. Therefore, they usually

have a pH higher than 7.5, as in LN1 [40]. On the contrary, the pH value is usually less than 6.5 when the leachate is young. In the case of the LN2 zone, the pH range is between 6.5 and 8.3. Therefore, an increase in pH may be because it has reached a state where there is a stabilization of the acid production processes [37].

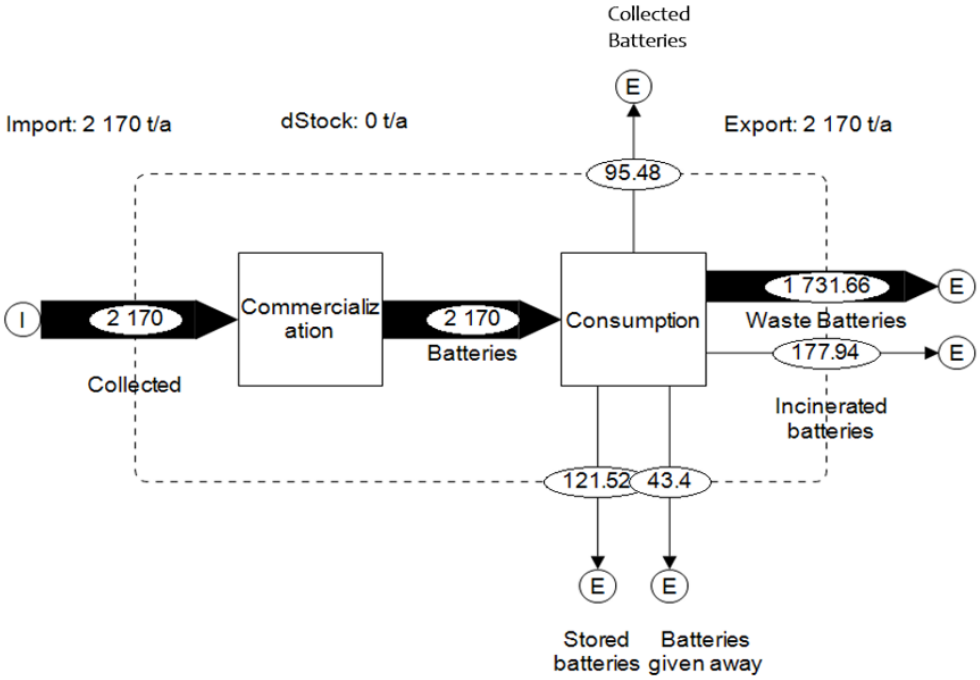

Figure 7. MFA of used batteries as disposal.

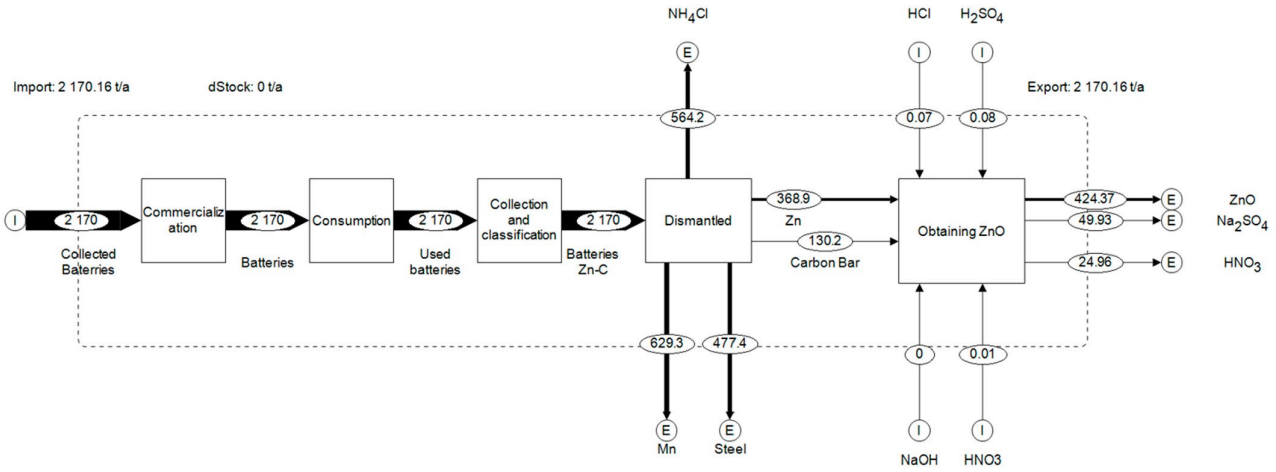

Figure 8. MFA of used batteries as a source of recycled metal.

The Zn concentrations measured in the LN1 and LN2 do not exceed 10,000 ug/L as seen in Table 5, thus remaining within the ranges regulated by the enforcement environmental entity. However, it is known that Zn accumulation can become toxic. Some symptoms of zinc poisoning include fever, breathing difficulty, nausea, chest pain, cough, gastric distress, dizziness, headaches, and loss of appetite. Furthermore, severe toxicity may cause copper deficiency anemia and hematological and neurological abnormalities [41,42].

Table 5. Zn concentration in leachates.

Metal	LN1, μgL^{-1}	LN2, μgL^{-1}	Standard, μgL^{-1}
Zn	500.89	1229	100.00

Zinc accumulation can be transferred by various means, such as water, soil, and plants. In turn, they can enter human bodies by food chains or by direct ingestion. This would pose a threat to human health [43]. The ingestion of very high doses of zinc can cause pulmonary lesions, necrosis in the bone marrow, liver, kidneys, and ocular lesions [37].

The data from the second MFA analysis are presented in Figure 8. The input data used were the same as in the first MFA. However, instead of the used batteries being discarded, incinerated, or stored at home after consumption, a process of recovery of zinc from the batteries was performed to obtain zinc oxide. In addition, we took advantage of the other components of the batteries to give them other uses. For this purpose, information was collected from each of the components of the battery, as shown in Table 2.

In this case, as shown in Figure 8, after storage, each component of the battery is separated. The different parts can be reused; for example, Mn can be used as an additive in ceramics. The amount of Zn was 369.9 t/y and the amount of carbon rod was 130.2 t/y. From this, the amount of ZnO that could be obtained was 424.37 t/y, thus enabling the recovery of a large part of the zinc compared to the number of batteries that ended up in the landfill. In addition to obtaining ZnO, $NaSO_4$ could also be obtained with 49.93 t/y and HNO_3 with 24.96 t/y. Therefore, these substances can be put to other uses instead of being disposed of. This whole process seeks to reuse all the components and substances produced both in the dismantling process and for obtaining ZnO.

This process aims to achieve the environmentally friendly recovery of metals, particularly zinc (Zn). This approach aims to minimize environmental and human health impacts, as evidenced by the reduced levels observed. Generally, the extraction of zinc is usually performed together with other metals, such as lead, which is known as one of the most toxic elements. Its extraction process is usually performed in an open pit. Therefore, there is a greater impact on the environment, especially due to the destruction of native flora and fauna. In addition, zinc must be separated from other materials, thus energy consumption is higher. Furthermore, smelting processes are carried out, in which harmful gases are produced, destroying the ecosystem through atmospheric pollution, and the solid waste generated ends up in the soil and in water sources [44,45].

3.3. Cooking Oil Processing and Characterization

The process for obtaining recycled cooking oil is provided by ETAPA EP, in which it is subjected to filtering, washing, and drying, as described in Section 2.1. The treated cooking oil was characterized to determine its density, viscosity, and water content. The results of the analysis are presented in Table 6. The density of the oil was found to be 0.9646 gcm^{-3}, which is consistent with the values reported in previous studies such as [46] (0.921 gcm^{-3}) and [47] (0.9119 gcm^{-3}). Furthermore, the density value is close to the ASTM D 1298 normative value of 0.96 gcm^{-3}. The viscosity of the oil was determined to be 50.9117 mm^2s^{-1}, which agrees with the viscosity values reported in similar studies, that is, (42.2 mm^2s^{-1}) [47] and (50 mm^2s^{-1}) [48]. The amount of water present in the sample was found to be 0.15%.

Table 6. Characteristics of recycled cooking oil.

Oil Characterization	
Density, gcm^{-3}	0.965
Viscosity, mm^2s^{-1}	50.912
Water amount, %	0.15

Figure 9 presents the results of fatty acids methyl esters (FAME) determined using GC-FID. The dominant fatty acid is C18:3 (α-linoleic acid), accounting for 30.54%. Therefore, all stoichiometric calculations were based on this fatty acid.

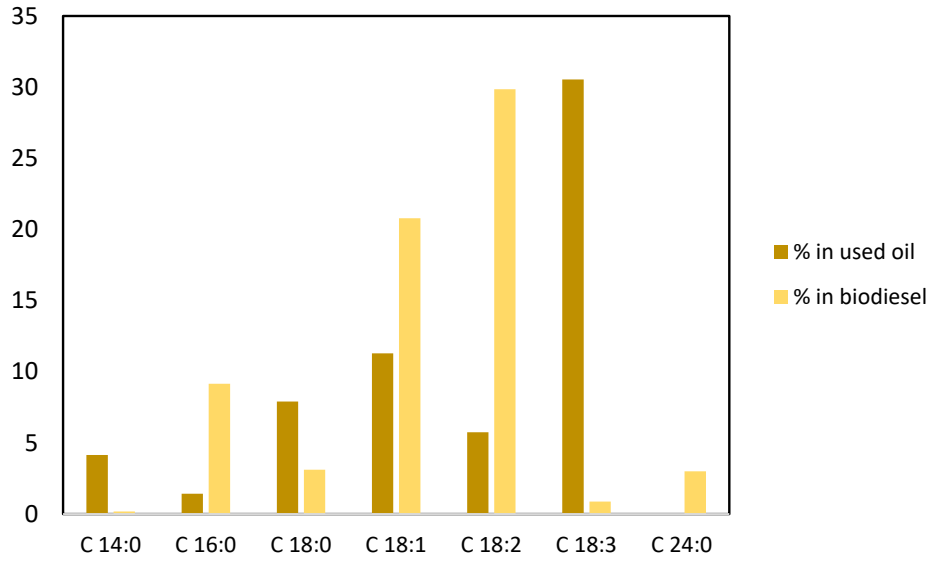

Figure 9. Fatty acids of used recycled cooking oil and biodiesel.

3.4. Biodiesel

In Figure 9 FAME composition is shown in percentage and g/mol. We can observe that the fatty acid in greater percentage is C18:2 (linoleic acid) accounting for 29.86%.

The results of the prepared biodiesel are shown in Table 7. The heating power for the prepared biodiesel is a little higher than values in other research, that is, between 35.9 kJg^{-1} to 37.26 kJg^{-1} [48,49]. This fact can be attributed to the catalyst, because zinc oxide boosts heating power in car engines [49]. The density obtained is within the range of 0.89 gcm^{-3} to 0.9 gcm^{-3}, as established by the INEN 148. The blank density was 0.93 gcm^{-3} in value, which is closer to the density of cooking oil. Therefore, without the use of the catalyst, the conversion was low. The viscosity obtained aligns with the ranges established by the INEN 2482, ASTM B 100, and EN 590 standards. The blank achieved higher viscosity than the norm, indicating that the transesterification was incomplete [50]. The water content is within the range of the INEN 2482, ASTM B 100, and EN 59 standards, demonstrating the effectiveness of the cooking oil drying process. The yield was 70.91%, surpassing the value of 49.78% registered in research that used the same catalyst [51]. However, compared to homogeneous catalysis that employed potassium hydroxide and calcium hydroxide, the achieved yield was lower, with yields ranging between 92% and 98% [28,52,53].

Table 7. Characteristics of biodiesel.

Biodiesel Characterization	
Heating power, kJg^{-1}	37.553
Density, gcm^{-3}	0.892
Viscosity, mm^2s^{-1}	4.189
Water amount, %	0.001
Yield, %	70.91

Despite obtaining better yields with other catalysts, zinc oxide is considered the most suitable catalyst for producing biodiesel due to its ability to reduce the time and temperature required for the synthesis [54]. Additionally, zinc oxide is a heterogeneous catalyst that can be easily recovered and does not require additional processes to neutralize

the final product. Moreover, the performance can be improved by adding other catalytic phases [55].

Figure 10 presents the process of obtaining biodiesel from used oil using a recycled catalyst. In Cuenca, it is possible to collect ~38 kg of batteries and ~40 gallons of used vegetal cooking oil per month, from which 0.984 kg of zinc oxide and 886 L of biodiesel could be obtained. The process begins by disassembling the collected batteries, and the zinc plate is then leached with a mixture of acids. The resulting mixture is filtered, neutralized, and precipitated to recover the oxide. The recycled oil is then washed and filtered to remove impurities. The biodiesel is produced from the mixture of the resulting oxide, the prepared oil, and ethanol by transesterification. The final product is decanted to separate the biodiesel and glycerin.

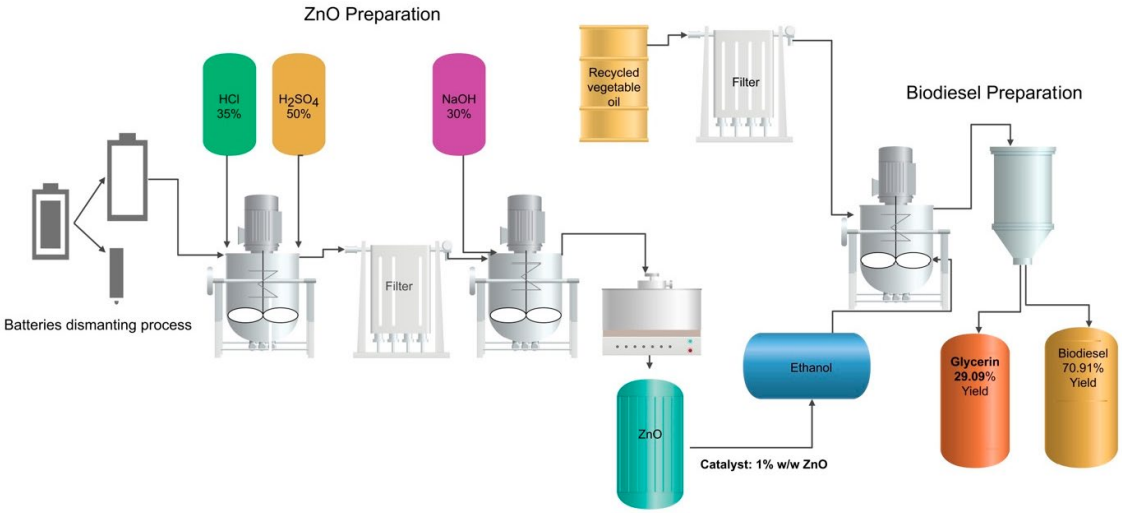

Figure 10. Scheme of the full process.

4. Conclusions

Obtaining biodiesel from recycled materials is a crucial step towards efficiently managing urban waste produced in Cuenca. If successful, this process could bring monetary benefits to ETAPA EP and promote the concept of a circular economy. This study transformed two wastes which are considered environmental liabilities into value-added products. Zinc oxide was obtained from zinc–carbon batteries, yielding 56% and a purity of 98%. A 5% zinc oxide catalyst was supported on a carbon rod, also recycled from the stack. The recycled oil was conditioned and characterized; it was determined that the fatty acid in major percentage was linoleic acid (18:2), 11.29%. The water amount was 0.15%, showing that the drying of the sample was effective. The density was 0.965 gcm^{-3} and the viscosity was determined to be 50.912 mm^2s^{-1}. Both parameters were within ASTM standards for recycled oils used to produce biodiesel. Better results for obtaining biodiesel with the pretreated vegetable oil and ethanol in a 6:1 ratio were obtained using the supported catalyst. The determination of the amount of water, viscosity, and density was the same as in the case of oil, obtaining the following values 0.005%, 0.892 gcm^{-3}, and 4.1887 mm^2s^{-1}, respectively. These parameters are within the ranges determined by biodiesel standards INEN 2482, ASTM B 100, and EN 590. The catalyst obtained favored the generation of biodiesel from recycled vegetable oil and ethanol. This was evidenced in the reaction yield since when using it, since a yield of 70.91% was obtained compared to the non-catalyzed blank where the yield was 0.5%. When comparing the yields between the catalyzed reactions, the yield and viscosity were not significantly different; the differences were found in terms of density. The supported catalyst allowed easier recovery of the catalyst.

The production of biodiesel involves several processes such as the production of zinc oxide, carbon treatment, and oil treatment. The energy consumption of each of the involved processes has been evaluated and quantified, resulting in an energy consumption of 32.9 kWh for obtaining the catalyst and 4.25 kWh for the oil treatment, thus obtaining the biodiesel sample through the reaction, which gives a total of 37.15 kWh.

Author Contributions: Conceptualization, V.P.-V. methodology, D.S.-C., M.O.-M. and V.P.-V.; software, D.S.-C. and M.O.-M.; validation, J.C.; investigation, D.S.-C. and M.O.-M.; resources, P.D.-S.; writing—original draft preparation, D.S.-C., M.O.-M. and V.P.-V., writing—review and editing, A.M.-I., J.C., P.Á.-L., P.D.-S., P.E.-P. and V.P.-V.; supervision, V.P.-V. All authors have read and agreed to the published version of the manuscript.

Funding: This research received no external funding.

Data Availability Statement: Not Applicable.

Conflicts of Interest: The authors declare no conflict of interest.

References

1. INEC. Información Ambiental en Los Hogares 2020. Available online: https://www.ecuadorencifras.gob.ec/documentos/web-inec/Encuestas_Ambientales/Hogares/Hogares-2022/MOD_AMB_HOGAR_ENEMDU_2022.pdf (accessed on 26 May 2023).
2. Ebin, B.; Petranikova, M.; Steenari, B.-M.; Ekberg, C. Investigation of Zinc Recovery by Hydrogen Reduction Assisted Pyrolysis of Alkaline and Zinc-Carbon Battery Waste. *Waste Manag.* **2017**, *68*, 508–517. [CrossRef]
3. Farzana, R.; Rajarao, R.; Behera, P.R.; Hassan, K.; Sahajwalla, V. Zinc Oxide Nanoparticles from Waste Zn-C Battery via Thermal Route: Characterization and Properties. *Nanomaterials* **2018**, *8*, 717. [CrossRef]
4. Mahandra, H.; Singh, R.; Gupta, B. Recycling of Zn-C and Ni-Cd Spent Batteries Using Cyphos IL 104 via Hydrometallurgical Route. *J. Clean. Prod.* **2018**, *172*, 133–142. [CrossRef]
5. INEN. Disposición de Productos Pilas y Baterias En Desuso, Requisitos. 2011. Available online: https://www.normalizacion.gob.ec/buzon/normas23/2534.pdf (accessed on 26 May 2023).
6. Abid Charef, S.; Affoune, A.M.; Caballero, A.; Cruz-Yusta, M.; Morales, J. Simultaneous Recovery of Zn and Mn from Used Batteries in Acidic and Alkaline Mediums: A Comparative Study. *Waste Manag.* **2017**, *68*, 518–526. [CrossRef]
7. Chicaiza, O. Programa de Gestión de Pilas Usadas. 2021. Available online: https://documentosboletinoficial.buenosaires.gob.ar/publico/PE-DIS-MAYEPGC-DGPOLEA-49-19-ANX.pdf (accessed on 26 May 2023).
8. Viswanathan, B. Chapter 12—Batteries. In *Energy Sources*; Viswanathan, B., Ed.; Elsevier: Amsterdam, The Netherlands, 2017; pp. 263–313. ISBN 978-0-444-56353-8.
9. Chen, W.-S.; Liao, C.-T.; Lin, K.-Y. Recovery Zinc and Manganese from Spent Battery Powder by Hydrometallurgical Route. *Energy Procedia* **2017**, *107*, 167–174. [CrossRef]
10. Tanong, K.; Tran, L.-H.; Mercier, G.; Blais, J.-F. Recovery of Zn (II), Mn (II), Cd (II) and Ni (II) from the Unsorted Spent Batteries Using Solvent Extraction, Electrodeposition and Precipitation Methods. *J. Clean. Prod.* **2017**, *148*, 233–244. [CrossRef]
11. Padoan, E.; Hernandez Kath, A.; Vahl, L.C.; Ajmone-Marsan, F. Potential Release of Zinc and Cadmium From Mine-Affected Soils Under Flooding, a Mesocosm Study. *Arch. Environ. Contam. Toxicol.* **2020**, *79*, 421–434. [CrossRef]
12. Zhang, X.; Yang, L.; Li, Y.; Li, H.; Wang, W.; Ye, B. Impacts of Lead/Zinc Mining and Smelting on the Environment and Human Health in China. *Environ. Monit. Assess.* **2012**, *184*, 2261–2273. [CrossRef] [PubMed]
13. Tao, M.; Zhang, X.; Wang, S.; Cao, W.; Jiang, Y. Life Cycle Assessment on Lead–Zinc Ore Mining and Beneficiation in China. *J. Clean. Prod.* **2019**, *237*, 117833. [CrossRef]
14. Ćwieląg-Drabek, M.; Piekut, A.; Gut, K.; Grabowski, M. Risk of Cadmium, Lead and Zinc Exposure from Consumption of Vegetables Produced in Areas with Mining and Smelting Past. *Sci. Rep.* **2020**, *10*, 3363. [CrossRef]
15. Oviedo Anchundia, R.; Moína-Quimí, E.; Naranjo-Morán, J.; Barcos-Arias, M. Contaminación Por Metales Pesados En El Sur Del Ecuador Asociada a La Actividad Minera. *Bionatura* **2017**, *2*, 437–441. [CrossRef]
16. Jia, Y.; Zhang, T.; Zhai, Y.; Bai, Y.; Ren, K.; Shen, X.; Cheng, Z.; Zhou, X.; Hong, J. Exploring the Potential Health and Ecological Damage of Lead–Zinc Production Activities in China: A Life Cycle Assessment Perspective. *J. Clean. Prod.* **2022**, *381*, 135218. [CrossRef]
17. Elgharbawy, A.S.; Sadik, W.A.; Sadek, O.M.; Kasaby, M.A.; Elgharbawy, A.S.; Sadik, W.A.; Sadek, O.M.; Kasaby, M.A. A review on biodiesel feedstocks and production technologies. *J. Chil. Chem. Soc.* **2021**, *66*, 5098–5109. [CrossRef]
18. Collin, T.; Cunningham, R.; Jefferson, B.; Villa, R. Characterisation and Energy Assessment of Fats, Oils and Greases (FOG) Waste at Catchment Level. *Waste Manag.* **2020**, *103*, 399–406. [CrossRef]
19. Chicaiza, O. Programa de Gestión de Aceite Vegetal. 2021.
20. Vásconez, L. Convenios en Cinco Ciudades del Ecuador Para Reciclar Aceites Usados. Available online: https://www.elcomercio.com/actualidad/ecuador/convenios-ciudades-ecuador-reciclar-aceites.html (accessed on 1 September 2021).

21. Bardhan, P.; Deka, A.; Bhattacharya, S.S.; Mandal, M.; Kataki, R. Chapter 18—Economical Aspect in Biomass to Biofuel Production. In *Value-Chain of Biofuels*; Yusup, S., Rashidi, N.A., Eds.; Elsevier: Amsterdam, The Netherlands, 2022; pp. 395–427. ISBN 978-0-12-824388-6.
22. Topi, D. Transforming Waste Vegetable Oils to Biodiesel, Establishing of a Waste Oil Management System in Albania. *SN Appl. Sci.* **2020**, *2*, 513. [CrossRef]
23. Neupane, D. Biofuels from Renewable Sources, a Potential Option for Biodiesel Production. *Bioengineering* **2023**, *10*, 29. [CrossRef]
24. Sheehan, J.; Camobreco, V.; Duffield, J.; Graboski, M.; Shapouri, H. *An Overview of Biodiesel and Petroleum Diesel Life Cycles*; National Renewable Energy Laboratory (U.S.): Golden, CO, USA, 2000; p. 60. [CrossRef]
25. Hamza, B.; Rouan, M.; Hammi, M.; Ziat, Y.; Chigr, M. Synthesis of Biodiesel by Transesterification of Used Frying Oils (UFO) through Basic Homogeneous Catalysts (NaOH and KOH). *Biointerface Res. Appl. Chem.* **2021**, *11*, 12858–12868. [CrossRef]
26. Sierra-Cantor, J.F.; Parra-Santiago, J.J.; Guerrero-Fajardo, C.A. Leaching and Reusing Analysis of Calcium–Zinc Mixed Oxides as Heterogeneous Catalysts in the Biodiesel Production from Refined Palm Oil. *Int. J. Environ. Sci. Technol.* **2019**, *16*, 643–654. [CrossRef]
27. Ramírez, J.; Buestán, L.; López-Maldonado, E.A.; Pinos-Vélez, V. Preparation and Physicochemical Characterization of Biodiesel from Recycled Vegetable Oil in Cuenca, Ecuador by Transesterification Catalyzed by KOH and NaOH. *Eng* **2023**, *4*, 954–963. [CrossRef]
28. Sipayung, R. Budiyono Optimization of Biodiesel Production from Used Cooking Oil Using Modified Calcium Oxide as Catalyst and N-Hexane as Solvent. *Mater. Today Proc.* **2022**, *63*, S32–S39. [CrossRef]
29. Yusuff, A.S.; Bhonsle, A.K.; Trivedi, J.; Bangwal, D.P.; Singh, L.P.; Atray, N. Synthesis and Characterization of Coal Fly Ash Supported Zinc Oxide Catalyst for Biodiesel Production Using Used Cooking Oil as Feed. *Renew. Energy* **2021**, *170*, 302–314. [CrossRef]
30. Hossain, M.N.; Siddik Bhuyan, M.S.U.; Md Ashraful Alam, A.H.; Seo, Y.C. Optimization of Biodiesel Production from Waste Cooking Oil Using S–TiO_2/SBA-15 Heterogeneous Acid Catalyst. *Catalysts* **2019**, *9*, 67. [CrossRef]
31. Chuquichanga, E.; León, D. Obtención de Óxido de Zinc a Partir de Pilas Zinc Carbono Desechables. Perú. 2019. Available online: http://repositorio.unac.edu.pe/handle/20.500.12952/4293 (accessed on 14 March 2023).
32. Samadhi, T. Environmental Impact of Sodium Sulfate Decomposition in Silicate Glass Manufacturing. Ph.D. Thesis, Alfred University, Alfred, NY, USA, 2003.
33. HERA. Cover Note of Sodium Sulfate. 2006. Available online: https://www.heraproject.com/files/39-f-06_sodium_sulfate_human_and_environmental_risk_assessment_v2.pdf (accessed on 26 May 2023).
34. INEN Biodiesel. Requisitos. 2013. Available online: https://www.normalizacion.gob.ec/buzon/normas23/2482.pdf (accessed on 26 May 2023).
35. ASTM Chapter 5 | Biodiesel. Available online: https://www.astm.org/mnl120170046.html (accessed on 4 January 2022).
36. EN Combustibles Para Automoción. Combustibles Par. Available online: https://www.une.org/encuentra-tu-norma/busca-tu-norma/norma/?c=N0052852 (accessed on 31 August 2022).
37. Alvarado, E.; GONZALES, K.; Mendoza, O. *Propuesta de un Método para la Recuperación de Zinc de Pilas Alcalinas Usadas bajo el Enfoque de Producción más Limpia*; Universidad de El Salvador: San Salvador, El Salvador, 2010.
38. ITC Trade Map—Estadísticas Del Comercio Para El Desarrollo Internacional de Las Empresas. Available online: https://www.trademap.org/Index.aspx (accessed on 2 March 2023).
39. INEC. Informacion Ambiental En Hogares 2022. Available online: https://www.ecuadorencifras.gob.ec/documentos/web-inec/Encuestas_Ambientales/Hogares/Hogares-2022/MOD_AMB_HOGAR_ENEMDU_2022.pdf (accessed on 1 March 2023).
40. Agbemafle, R.; Aggor-Woananu, S.E.; Akutey, O.; Bentum, J. Heavy Metal Concentrations in Leachates and Crops Grown Around Waste Dumpsites in Sekondi-Takoradi in the Western Region of Ghana. *Res. J. Environ. Toxicol.* **2019**, *14*, 16–25. [CrossRef]
41. Hussain, S.; Khan, M.; Sheikh, T.M.M.; Mumtaz, M.Z.; Chohan, T.A.; Shamim, S.; Liu, Y. Zinc Essentiality, Toxicity, and Its Bacterial Bioremediation: A Comprehensive Insight. *Front. Microbiol.* **2022**, *13*, 900740. [CrossRef]
42. Ryu, M.-S.; Aydemir, T.B. Chapter 23—Zinc. In *Present Knowledge in Nutrition*, 11th ed.; Marriott, B.P., Birt, D.F., Stallings, V.A., Yates, A.A., Eds.; Academic Press: Cambridge, MA, USA, 2020; pp. 393–408. ISBN 978-0-323-66162-1.
43. Kan, X.; Dong, Y.; Feng, L.; Zhou, M.; Hou, H. Contamination and Health Risk Assessment of Heavy Metals in China's Lead–Zinc Mine Tailings: A Meta–Analysis. *Chemosphere* **2021**, *267*, 128909. [CrossRef] [PubMed]
44. Du, B.; Zhang, H.; Ji, D.; Huang, Z.; Fangqun, G.; Zhou, J. Environmental Contamination and Health Risk Assessment to Toxic Elements in an Active Lead–Zinc Mining Area. *Expo. Health* **2022**, 1–12. [CrossRef]
45. Johansen, P.; Asmund, G.; Aastrup, P.; Tamstorf, M. *Environmental Impact of the Lead-Zinc Mine at Mestervig, East Greenland*; National Environmental Research Institute, University of Aarhus: Aarhus, Denmark, 2008.
46. López, L.; Bocanegra, J.; Malagón-Romero, D. Obtención de biodiesel por transesterificación de aceite de cocina usado. *Ing. Univ.* **2015**, *19*, 155–172. [CrossRef]
47. Rodriguez, D.; Riesco, J. Obtención de Biodiesel a Partir de Mezclas de Aceite de Cocina Usado y Aceite de Higuerilla Por Transesterificación. Available online: https://www.jovenesenlaciencia.ugto.mx/index.php/jovenesenlaciencia/article/view/1296 (accessed on 5 September 2022).

48. Tacias Pascacio, V.G.; Rosales Quintero, A.; Torrestiana Sánchez, B.; Tacias Pascacio, V.G.; Rosales Quintero, A.; Torrestiana Sánchez, B. Evaluación y caracterización de grasas y aceites residuales de cocina para la producción de biodiésel: Un caso de estudio. *Rev. Int. Contam. Ambient.* **2016**, *32*, 303–313. [CrossRef]
49. Gavhane, R.S.; Kate, A.M.; Pawar, A.; Safaei, M.R.; Soudagar, M.M.E.; Mujtaba Abbas, M.; Muhammad Ali, H.; Banapurmath, N.R.; Goodarzi, M.; Badruddin, I.A.; et al. Effect of Zinc Oxide Nano-Additives and Soybean Biodiesel at Varying Loads and Compression Ratios on VCR Diesel Engine Characteristics. *Symmetry* **2020**, *12*, 1042. [CrossRef]
50. Sánchez, E.M. Obtención de Biodiesel a Partir de Aceites Vegetales Empleando Catalizadores Sólidos Nanoestructurados. 2021. Available online: https://ria.utn.edu.ar/bitstream/handle/20.500.12272/5187/Tesis%20Doctoral%20-%20S%C3%A1nchez%20Faba%2C%20Edgar%20M.%20-%20UTN%20FRC.pdf?sequence=1&isAllowed=y (accessed on 24 March 2022).
51. Diaz, D.; Camargo, G.; Molano, M. Evaluación de Catalizadores de Óxido de Zinc y Su Actividad Catalítica En La Reacción de Transesterificación Para La Producción de Biodiésel. *Afinidad* **2008**, *65*, 299–305.
52. Fangfang, F.; Alagumalai, A.; Mahian, O. Sustainable Biodiesel Production from Waste Cooking Oil: ANN Modeling and Environmental Factor Assessment. *Sustain. Energy Technol. Assess.* **2021**, *46*, 101265. [CrossRef]
53. Sivarethinamohan, S.; Hanumanthu, J.R.; Gaddam, K.; Ravindiran, G.; Alagumalai, A. Towards Sustainable Biodiesel Production by Solar Intensification of Waste Cooking Oil and Engine Parameter Assessment Studies. *Sci. Total Environ.* **2022**, *804*, 150236. [CrossRef]
54. Dasta, P.; Pratap Singh, A.; Pratap Singh, A. Zinc Oxide Nanoparticle as a Heterogeneous Catalyst in Generation of Biodiesel. *Mater. Today Proc.* **2022**, *52*, 751–757. [CrossRef]
55. Guo, M.; Jiang, W.; Ding, J.; Lu, J. Highly Active and Recyclable CuO/ZnO as Photocatalyst for Transesterification of Waste Cooking Oil to Biodiesel and the Kinetics. *Fuel* **2022**, *315*, 123254. [CrossRef]